Journal of Solid and Fluid Mechanics (JSFM), 13(3): 1-5, 2023

Shahrood University of Technology

Journal of Solid and Fluid Mechanics (JSFM)

DOI: 10.22044/JSFM.2023.13043.3734

Manufacturing Engineering of Iran

Unbalance response of a spinning pipe conveying fluid in vertical configuration equipped with piezoelectric patches

Reza Ebrahimi

Assist. Prof. of Mechanical Engineering, Faculty of Engineering, Yasouj University, Yasouj, Iran

*Corresponding author: rebrahimi@yu.ac.ir

Received: 04/30/2023 Revised: 06/21/2023 Accepted: 08/19/2023

Abstract

There are many engineering applications of pipes at different scales for conveying fluid. The dynamic characteristics of a spinning pipe conveying fluid in vertical configuration equipped with piezoelectric patches are analyzed in this study. Based on Euler–Bernoulli beam theory, the governing equations of the system are derived by applying Hamilton's variational principle. In this equations, the gyroscopic coupling, electromechanical coupling and gravitational effects are considered. The Galerkin's method is used to discretize the governing equations of motions. Numerical results are investigated to predict the influences of the piezoelectric layer spanning angle, spinning speed, pipe length and flow velocity, on the unbalance response of the system. The results indicate that, depending on excitation frequency, the vibration amplitude can be decreased or increased by increasing the piezoelectric layer spanning angle. The results of this research can be used to conduct piezoelectric pipe design and performance predictions for future pipe vibration control and energy harvesting applications.

Keywords: Spinning pipe, Vertical configuration, Piezoelectric, Fluid–structure interaction, Vibration, Unbalance response.

1. Introduction

As a significant aspect of fluid-structure interaction (FSI), flow-induced vibrations of pipes conveying fluid have attracted much attention due to the wide applications of these pipes in various engineering fields, such as drug delivery, agriculture, heat exchangers and drill strings [1]. Numerous researches have been carried out on the vibrational behavior of pipes conveying fluid.

Kheiri et al. [2] studied dynamics and stability of a pipe flexibly supported at its ends and conveying fluid. The results showed that there are ranges of support stiffness in which the critical flow velocity stays constant with changing the support stiffnesses.

Pisarski et al. [3] proposed a mathematical model of a fluid-conveying pipe actuated by the electromechanical damper. They found that the combined effects of the additional mass and the viscous-type electromagnetic force can improve dynamic stability the cantilever pipe discharging fluid.

Elvin and Elvin [4] investigated the dynamic stability of a cantilever pipe with attached piezoelectric resistive dampers. The results showed that a greater piezoelectric electromechanical coupling coefficient tends to increase the critical flutter speed due to the increased in electromechanical coupling stiffness.

Abbasnejad et al. [5] analyzed the effect of applying piezoelectric layers on stability of the fluid conveying micro-pipes. They revealed that imposing voltage difference to piezoelectric layers can significantly suppress the effect of fluid flow on vibrational frequencies and thus extend the stable margins.

Liang et al. [6] analyzed transverse free vibration and stability of spinning pipes conveying fluid. They reported that the qualitative stability of spinning pipes conveying fluid mainly depends on the effect of FSI, while the spinning speed has a great influence on the quantitative values of the frequency.

From the review of literature, it is found that there is no previously published work presenting unbalance response of pipes conveying fluid that incorporates the spinning motion, the gyroscopic coupling of the nonplanar vibrations, the electromechanical coupling and the gravitational effects due to the vertical installation. Therefore, in this study the effects of different parameters on the frequency response of the vertically spinning cantilevered pipe conveying fluid with surface mounted piezoelectric layer are investigated.

2. Formulation of the governing equations

Figure 1 shows the model of a vertically spinning cantilevered pipe conveying fluid with surface mounted piezoelectric layer. The pipe has a uniform cross

section. The flow velocity U_0 of the internal fluid is constant and the velocity profile is uniform.

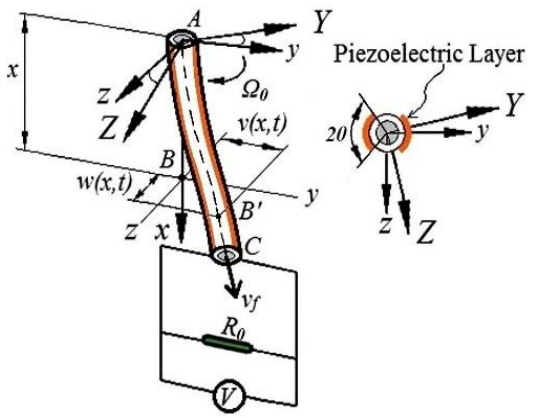

Figure 1. Schematic diagram of a vertically spinning cantilevered pipe conveying fluid with surface mounted piezoelectric layer.

The pipe unbalance is purely static with radius e (Figure 2). The piezoelectric patch pair is bonded to the surface of the pipe at the top and the bottom of the z-axis. The top and the bottom piezoelectric layer are connected in series with the same polarization. The electrical circuit of the piezoelectric layer consists of a resistive load R_0.

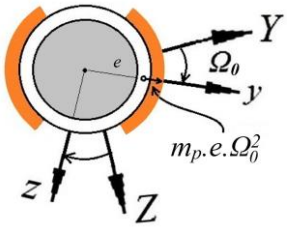

Figure 2. Cross section of the piezoelectric pipe with unbalance force

By applying Hamilton's variational principle and introducing the nondimensional parameters given in Table 1, the coupled nonlinear partial differential equations of motion are found to be

$$\begin{aligned}
&\frac{\partial^4 \mathrm{v}(\mathrm{x},\mathrm{t})}{\partial \mathrm{x}^4}+\frac{\partial^2 \mathrm{v}(\mathrm{x},\mathrm{t})}{\partial \mathrm{t}^2}+C\frac{\partial \mathrm{v}(\mathrm{x},\mathrm{t})}{\partial \mathrm{t}}\\
&+2mU\frac{\partial^2 \mathrm{v}(\mathrm{x},\mathrm{t})}{\partial \mathrm{t}\partial \mathrm{x}}+mU^2\frac{\partial^2 \mathrm{v}(\mathrm{x},\mathrm{t})}{\partial \mathrm{x}^2}\\
&-2mU\omega\frac{\partial \mathrm{w}(\mathrm{x},\mathrm{t})}{\partial \mathrm{x}}-2\omega\frac{\partial \mathrm{w}(\mathrm{x},\mathrm{t})}{\partial \mathrm{t}}\\
&-\omega^2 \mathrm{v}(\mathrm{x},\mathrm{t})+g\left(\frac{\partial \mathrm{v}(\mathrm{x},\mathrm{t})}{\partial \mathrm{x}}\right.\\
&\left.-(1-\mathrm{x})\frac{\partial^2 \mathrm{v}(\mathrm{x},\mathrm{t})}{\partial \mathrm{x}^2}\right)\\
&+\mathrm{V}(\mathrm{t})\left(\delta'(\mathrm{x})-\delta'(\mathrm{x}-1)\right)\\
&+mU\left(\frac{\partial \mathrm{v}(\mathrm{x},\mathrm{t})}{\partial \mathrm{t}}-\omega \mathrm{w}(\mathrm{x},\mathrm{t})\right.\\
&\left.+U\frac{\partial \mathrm{v}(\mathrm{x},\mathrm{t})}{\partial \mathrm{x}}\right)\delta(\mathrm{x}-1)-F=0
\end{aligned} \tag{1}$$

$$\begin{aligned}
&\frac{\partial^4 \mathrm{w}(\mathrm{x},\mathrm{t})}{\partial \mathrm{x}^4}+\frac{\partial^2 \mathrm{w}(\mathrm{x},\mathrm{t})}{\partial \mathrm{t}^2}+C\frac{\partial \mathrm{w}(\mathrm{x},\mathrm{t})}{\partial \mathrm{t}}\\
&+2mU\frac{\partial^2 \mathrm{w}(\mathrm{x},\mathrm{t})}{\partial \mathrm{t}\partial \mathrm{x}}+mU^2\frac{\partial^2 \mathrm{w}(\mathrm{x},\mathrm{t})}{\partial \mathrm{x}^2}\\
&+2mU\omega\frac{\partial \mathrm{v}(\mathrm{x},\mathrm{t})}{\partial \mathrm{x}}+2\omega\frac{\partial \mathrm{v}(\mathrm{x},\mathrm{t})}{\partial \mathrm{t}}\\
&-\omega^2 \mathrm{w}(\mathrm{x},\mathrm{t})+g\left(\frac{\partial \mathrm{w}(\mathrm{x},\mathrm{t})}{\partial \mathrm{x}}\right.\\
&\left.-(1-\mathrm{x})\frac{\partial^2 \mathrm{w}(\mathrm{x},\mathrm{t})}{\partial \mathrm{x}^2}\right)\\
&+mU\left(\frac{\partial \mathrm{w}(\mathrm{x},\mathrm{t})}{\partial \mathrm{t}}+\omega \mathrm{v}(\mathrm{x},\mathrm{t})\right.\\
&\left.+U\frac{\partial \mathrm{w}(\mathrm{x},\mathrm{t})}{\partial \mathrm{x}}\right)\delta(\mathrm{x}-1)=0
\end{aligned} \tag{2}$$

$$\eta\frac{d\mathrm{V}(\mathrm{t})}{d\mathrm{t}}+\frac{\mathrm{V}(\mathrm{t})}{R}-\frac{\partial^2 \mathrm{v}(\mathrm{x},\mathrm{t})}{\partial \mathrm{t}\partial \mathrm{x}}\delta(\mathrm{x}-1)=0 \tag{3}$$

3. Galerkin's discretization

The Galerkin's procedure based on the two mode approximation is employed for converting the partial differential equations to the ordinary differential equations. So, the deflection functions are approximated by the series

$$\begin{aligned}
\mathrm{v}(\mathrm{x},\mathrm{t}) &= \sum_{k=1}^{2}\varphi_k(\mathrm{x})q_{\mathrm{v}_k}(\mathrm{t})\\
&= [\Phi(\mathrm{x})]^T[q_{\mathrm{v}}(\mathrm{t})]
\end{aligned} \tag{4}$$

$$\begin{aligned}
\mathrm{w}(\mathrm{x},\mathrm{t}) &= \sum_{k=1}^{2}\varphi_k(\mathrm{x})q_{\mathrm{w}_k}(\mathrm{t})\\
&= [\Phi(\mathrm{x})]^T[q_{\mathrm{w}}(\mathrm{t})]
\end{aligned} \tag{5}$$

Substitution of Eqs. (4) and (5) into Eqs. (1)-(3), followed by multiplication by [Φ] and integration over

the domain (*0, 1*) yields

$$[\ddot{q}_{\mathrm{v}}(\mathrm{t})]+[\Gamma_1][\dot{q}_{\mathrm{v}}(\mathrm{t})]-[\Gamma_2][\dot{q}_{\mathrm{w}}(\mathrm{t})] -[\Gamma_3][q_{\mathrm{w}}(\mathrm{t})]+[\Gamma_4][q_{\mathrm{v}}(\mathrm{t})] +[\Gamma_5]\mathrm{V}(\mathrm{t})=0 \quad (6)$$

$$[\ddot{q}_{\mathrm{w}}(\mathrm{t})]+[\Gamma_1][\dot{q}_{\mathrm{w}}(\mathrm{t})]+[\Gamma_2][\dot{q}_{\mathrm{v}}(\mathrm{t})] +[\Gamma_3][q_{\mathrm{v}}(\mathrm{t})]+[\Gamma_4][q_{\mathrm{w}}(\mathrm{t})]=0 \quad (7)$$

$$\eta\frac{d\mathrm{V}(\mathrm{t})}{d\mathrm{t}}+\frac{\mathrm{V}(\mathrm{t})}{R}-[\Gamma_5]^T[\dot{q}_{\mathrm{v}}(\mathrm{t})]=0 \quad (8)$$

For numerical analysis, it is convenient to transform Eqs. (6)-(8) into the first order differential equations as

$$[\dot{q}(\mathrm{t})]=[A][q(\mathrm{t})]+[B]u \quad (9)$$

$$[Y(\mathrm{t})]=[C][q(\mathrm{t})]+[D]u \quad (10)$$

The constant matrices *[A]*, *[B]*, *[C]*, *[D]*, *[Γ1]*, *[Γ2]* … and *[Γ5]* are defined in the Appendix.

Table 1. Dimensionless parameters

$$\mathrm{x}=\frac{x}{L} \qquad \mathrm{v}(\mathrm{x},\mathrm{t})=\frac{v(x,t)}{L}$$

$$\mathrm{w}(\mathrm{x},\mathrm{t})=\frac{w(x,t)}{L} \qquad \mathrm{V}(\mathrm{t})=\frac{e_{31}LI_{pz_1}V(t)}{2\left(E_pI_p+E_{pz}I_{pz_2}\right)}$$

$$\mathrm{t}=\frac{t}{L^2}\left(\frac{E_pI_p+E_{pz}I_{pz_2}}{m_p+m_f+m_{pz}}\right)^{\frac{1}{2}} \qquad R=\frac{R_0\left(e_{31}I_{pz_1}\right)^2}{4L\left(\left(E_pI_p+E_{pz}I_{pz_2}\right)\left(m_p+m_f+m_{pz}\right)\right)^{\frac{1}{2}}}$$

$$U=U_0L\left(\frac{m_p+m_f+m_{pz}}{E_pI_p+E_{pz}I_{pz_2}}\right)^{\frac{1}{2}} \qquad m=\frac{m_f}{m_p+m_f+m_{pz}}$$

$$\omega=\Omega_0L^2\left(\frac{m_p+m_f+m_{pz}}{E_pI_p+E_{pz}I_{pz_2}}\right)^{\frac{1}{2}} \qquad g=\frac{g_0L^3\left(m_p+m_f+m_{pz}\right)}{E_pI_p+E_{pz}I_{pz_2}}$$

$$\eta=\frac{4C_p\left(E_pI_p+E_{pz}I_{pz_2}\right)}{L\left(e_{31}I_{pz_1}\right)^2} \qquad R=\frac{R_0\left(e_{31}I_{pz_1}\right)^2}{4L\left(\left(E_pI_p+E_{pz}I_{pz_2}\right)\left(m_p+m_f+m_{pz}\right)\right)^{\frac{1}{2}}}$$

$$F=\frac{m_pL^3e\Omega^2}{\left(E_pI_p+E_{pz}I_{pz_2}\right)}$$

4. Results and discussion

In this section, the effects of some parameters on the vibration behavior of the spinning cantilevered piezoelectric pipe conveying fluid are inspected. Water is assumed as the fluid conveyed with a density of *1000* kg/m^3. The parameter values used in the analysis are presented in Table 2.

Table 2. Physical parameters of the piezoelectric pipe.

Parameter	Piezoelectric	Pipe
Material	PZT-5 H	Rubber
Density (*kg/m^3*)	*7500*	*1200*
Length (*mm*)	*50*	*50*
Thickness (*mm*)	*1*	*3.2*
Inner diameter (*mm*)	-	*12.7*
Young's modulus (*GPa*)	*60.6*	*0.4*
Piezoelectric constant (*C/m^2*)	*-16.6*	-
Piezoelectric permittivity (*nF/m*)	*25.55*	-
Spanning angle (*rad*)	*π/2*	-
Acceleration of gravity (*m/s^2*)	*9.81*	*9.81*

Figure 3 shows the non-dimensional frequency response of the system at various values of the flow velocity (U_0=*800*, *1000*, *3670*, *4000* and *4300* mm/s) for $\theta=\pi/2$ rad, L=*50* mm and Ω_0=*100* rpm. Two resonance peaks are observed in the frequency response of the system. The flow velocity has a considerable effect on the vibration behavior of the system at low frequencies, whereas at high frequencies, the effect of the flow velocity on the vibration behavior of the system decreases. It is clear from Figure 3 that, when the flow velocity is lower than the critical speed (U_0=*3670* mm/s), increasing the amount of flow velocity reduces the amplitude of vibration and enhances the first natural frequency. When the flow velocity exceeds the critical value (U_0=*3670* mm/s), increasing the amount of flow velocity enhances the amplitude of vibration and reduces the first natural frequency.

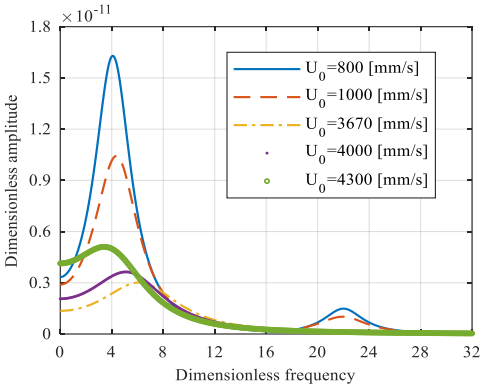

Figure 3. Dimensionless frequency response of the vertically spinning piezoelectric pipe conveying fluid at different flow velocities for $\theta=\pi/2$ rad, $L=50$ mm and $\Omega_0=100$ rpm

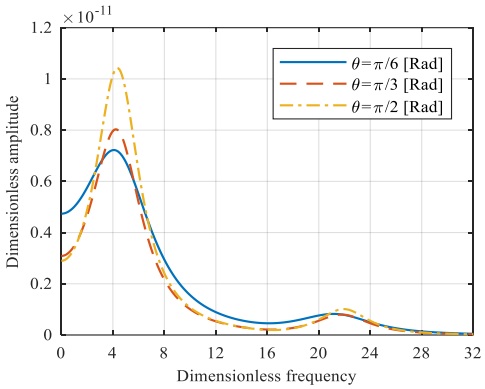

Figure 4. Dimensionless frequency response of the vertically spinning piezoelectric pipe conveying fluid at different spanning angles for $U_0=1000$ mm/s, $L=50$ mm and $\Omega_0=100$ rpm

Figure 4 depicts the non-dimensional frequency response of the system at various values of the spanning angle ($\theta=\pi/6$, $\pi/3$ and $\pi/2$ rad) for $U_0=1000$ mm/s, $L=50$ mm and $\Omega_0=100$ rpm. The results show that the natural frequencies increase with increase in the spanning angle. Also, at low frequencies, increasing the amount of spanning angle reduces the amplitude of vibration, whereas near the resonance frequencies, increasing the amount of spanning angle enhances the amplitude of vibration.

5. Conclusions

Some important conclusions that can be drawn from this work are:

- The first natural frequency can be enhanced by increasing the piezoelectric spanning angle.
- Increasing the spanning angle do not always lead to the higher vibration amplitude, and depending on the value of the excitation frequency.
- The first natural frequency can be increased (for subcritical flow velocities) or decreased (for supercritical flow velocities) by increasing the flow velocity.

6. Appendix

The constant matrices of Eqs. (6)- (10) are as follows:

$$[\Gamma_1]=C[\mathrm{I}]+2mU\int_0^1[\Phi(\mathrm{x})][\Phi'(\mathrm{x})]^T\,d\mathrm{x}+mU[\Phi(1)][\Phi(1)]^T$$

$$[\Gamma_2]=2\omega[\mathrm{I}]$$

$$[\Gamma_3]=mU\omega\left(2\int_0^1[\Phi(\mathrm{x})][\Phi'(\mathrm{x})]^T\,d\mathrm{x}+[\Phi(1)][\Phi(1)]^T\right)$$

$$[\Gamma_4]=\int_0^1[\Phi(\mathrm{x})][\Phi''''(\mathrm{x})]^T\,d\mathrm{x}+mU^2\int_0^1[\Phi(\mathrm{x})][\Phi''(\mathrm{x})]^T\,d\mathrm{x}-\omega^2[\mathrm{I}]+g\int_0^1\left([\Phi(\mathrm{x})][\Phi'(\mathrm{x})]^T-(1-\mathrm{x})[\Phi(\mathrm{x})][\Phi''(\mathrm{x})]^T\right)d\mathrm{x}+mU^2[\Phi(1)][\Phi'(1)]^T$$

$$[\Gamma_5]=[\Phi'(1)]$$

$$[\Gamma_6]=\int_0^1[\Phi(\mathrm{x})]d\mathrm{x}$$

$$[\Gamma_7]=[\Phi(1)]$$

$$[Y(\mathrm{t})]=\begin{bmatrix}\mathrm{v}(1,\mathrm{t})\\ \mathrm{w}(1,\mathrm{t})\\ \mathrm{V}(\mathrm{t})\end{bmatrix}$$

$$[q(\mathrm{t})]=\begin{bmatrix}[q_{\mathrm{v}}(\mathrm{t})]\\ [q_{\mathrm{w}}(\mathrm{t})]\\ \mathrm{V}(\mathrm{t})\\ [\dot{q}_{\mathrm{v}}(\mathrm{t})]\\ [\dot{q}_{\mathrm{w}}(\mathrm{t})]\end{bmatrix}$$

$$[A]=\begin{bmatrix}[0]_{2\times2} & [0]_{2\times2} & [0]_{2\times1} & [I]_{2\times2} & [0]_{2\times2}\\ [0]_{2\times2} & [0]_{2\times2} & [0]_{2\times1} & [0]_{2\times2} & [I]_{2\times2}\\ [0]_{1\times2} & [0]_{1\times2} & -\dfrac{1}{\eta R} & \dfrac{[\Gamma_5]^T}{\eta} & [0]_{1\times2}\\ -[\Gamma_4] & [\Gamma_3] & -[\Gamma_5] & -[\Gamma_1] & [\Gamma_2]\\ -[\Gamma_3] & -[\Gamma_4] & [0]_{2\times1} & -[\Gamma_2] & -[\Gamma_1]\end{bmatrix}$$

$$[B]=\begin{bmatrix}[0]_{2\times1}\\ [0]_{2\times1}\\ 0\\ [\Gamma_6]\\ [0]_{2\times1}\end{bmatrix}$$

$$[C]=\begin{bmatrix}[\Gamma_7]^T & [0]_{1\times2} & 0 & [0]_{1\times2} & [0]_{1\times2}\\ [0]_{1\times2} & [\Gamma_7]^T & 0 & [0]_{1\times2} & [0]_{1\times2}\\ [0]_{1\times2} & [0]_{1\times2} & 1 & [0]_{1\times2} & [0]_{1\times2}\end{bmatrix}$$

$$[D]=[0]_{3\times1}$$

7. References

[1] Païdoussis MP (2014) Fluid-structure interactions: slender structures and axial flow. *Academic Press*, London.

[2] Kheiri M, Païdoussis MP, Costa Del Pozo G, Amabili M (2014) Dynamics of a pipe conveying fluid flexibly restrained at the ends. *J Fluid Struct* 49: 360–385.

[3] Pisarski D, Konowrocki R, Szmidt T (2018) Dynamics and optimal control of an electromagnetically actuated cantilever pipe conveying fluid. *J. Sound Vib* 432: 420–436.

[4] Elvin NG, Elvin AA (2009) The flutter response of a piezoelectrically damped cantilever pipe. *J Intel Mat Syst Str* 20: 2017-2026.

[5] Abbasnejad B, Shabani R, Rezazadeh G (2015) Stability analysis of a piezoelectrically actuated micro‐pipe conveying fluid. *Microfluid Nanofluid* 19: 577–584.

[6] Liang F, Yang XD, Qian YJ, Zhang W (2018) Transverse free vibration and stability analysis of spinning pipes conveying fluid. *Int J Mech Sci* 137: 195–204.